



Nonlinear Buckling of Circular Nano Plates on Elastic Foundation

M. Jabbarzadeh*, M. Sadeghian

Department of Mechanical Engineering, Mashhad Branch, Islamic Azad University, Mashhad, Iran

PAPER INFO

Paper history:

Received 03 July 2015

Received in revised form 24 February 2016

Accepted 04 March 2016

Keywords:

Nonlinear Buckling

Circular

Orthotropic

Nonlocal Elasticity

Differential Quadrature Method

ABSTRACT

The following article investigates nonlinear symmetric buckling of moderately thick circular Nano plates with an orthotropic property under uniform radial compressive in-plane mechanical load. Taking into account Eringen nonlocal elasticity theory, principle of virtual work, first order shear deformation plate theory (FSDT) and nonlinear Von-Karman strains, the governing equations are obtained based on displacements. The differential quadrature method (DQM) as a numerical procedure is applied for solving the equations. In this analysis, for solving the stability equations, adjacent equilibrium method is employed. In nonlinear buckling analyses and for obtaining the buckling load, generally the available nonlinear terms of the stability equation are neglected. However, in this study, for getting the most accurate data, nonlinear terms are considered and the non-dimensional buckling load is compared with the condition of considering or neglecting that of terms and the effect of that of terms are also studied. The accuracy of the present results is validated by comparing the solutions with available studies. The effects of nonlocal parameter, thickness, radius and elastic foundation are investigated on non-dimensional buckling loads. The results of analyses based on local and non-local theories are compared. From the results, it can be seen that the effect of nonlocal parameter on simply support condition is less than clamped condition. It can be observed that with increasing the radius of the plate, the difference between local and non-local analyses, increases.

doi: 10.5829/idosi.ije.2016.29.05b.14

1. INTRODUCTION

Iijima played a significant role in materials science by introducing carbon nanotube [1] which was a starting point in the improvement of Nano science. Carbon nanostructured materials include graphene sheets and carbon nanotubes contain superior mechanical, electrical and chemical properties which make them uniquely practical in industrial and academic purposes such as battery manufacturing [2], chemical and biological sensors [3], solar cells [4] and etc. Except experimental methods, theoretical models such as atomistic methods are used for identifying the behavior and properties of Nano structures [5, 6].

The classical continuum mechanics models are scale free so their application becomes controversial in some papers. Thus, the traditional continuum mechanics

needs to be improved so that it could be utilized for investigating small scale structures [7]. Eringen proposed the nonlocal continuum elasticity taking into account the size effects and then accommodating the size-dependent phenomena [8]. In this theory, the stress at an arbitrary point is assumed to be function of the strain field at every point in the body. Meanwhile, the governing relations of Eringen nonlocal elasticity are relatively simple and small-scale effects in micro and nano-scale structures are considered. In this reason Continuum mechanics approaches are used for modeling structures [9, 10].

Numerous researches in the field of nano plates based on Eringen nonlocal theory have been done. Pradhan et al. [11], studied the buckling of rectangular single-layer graphene sheets with using nonlocal continuum mechanics and differential quadrature method (DQM). They showed that the rate of non-local parameter has significant impact on graphene sheets and reduces the buckling load. Samei et al. [12] presented

*Corresponding Author Email: jabbarzadeh@mshdiau.ac.ir (M. Jabbarzadeh)

the buckling response under load uniform isotropic rectangular graphene sheets with linear strains, analytically. Farajpour et al. [13] investigated the buckling of graphene plates with variable thickness and showed that the buckling behavior of monolayer graphene sheet strongly relies on the rate of nonlocal parameter. Farajpour and colleagues [14], investigated the buckling of rectangular orthotropic plates using DQM. Emam [15] presented a model for buckling and post-buckling nano beam theories such as first-order and higher-order and classic theory. Mohammadi et al. [16] investigated the buckling behavior of orthotropic rectangular single-layer nano plates on elastic foundation in thermal environment using DQM. Sarami and Azhari [17] analyzed the vibration and buckling of rectangular isotropic graphene plates using finite strips for various boundary conditions. From the research of Ravari and Shahidi [18], it can be seen that classical theory is used and the finite difference method for buckling of circular/annular nano plates is utilized. Bedroud et al. [19] studied symmetric and asymmetric buckling of thin isotropic nano-sheets, based on nonlocal elasticity and first order shear deformation theory with linear strains using exact closed-form solutions. Golmakani and Rezatalab [20] examined the nonlinear buckling of rectangular plates under non-uniform loads by using the first-order shear deformation theory, nonlinear strains and using DQM. Dastjerdi and Jabbarzadeh [21] tried to obtain an approximate single layer equivalent for multi-layer graphene sheets based on third order non-local elasticity theory. In their paper, results were obtained applying DQM, and then a new semi-analytical polynomial method (SAPM) was presented. Dastjerdi and Jabbarzadeh [22] investigated the nonlinear bending behavior of bilayer orthotropic rectangular graphene plate embedded in an elastic matrix with two parameters Winkler and Pasternak, based on the Eringen nonlocal elasticity theory using DQM. Dastjerdi et al. [23] studied the nonlinear bending analysis of annular/circular graphene sheet embedded in two parameter Winkler–Pasternak matrix applying the non-local elasticity theory. Farajpour et al. [24] studied axisymmetric buckling of the circular graphene sheets, using classical theory. They concluded that the nonlocal parameter has a significant role in the buckling of circular nano plate.

In this study, the buckling analysis of moderately thick circular orthotropic graphene sheets with non-linear strain under uniform radial load is analyzed. The effects of small scale are considered using non-local elasticity theory. The equilibrium equations are derived from the energy method and they were solved based on the adjacent equilibrium method. Also, differential quadrature is used as a numerical method. In nonlinear buckling analysis and for simplicity, after employing nonlinear strains to the buckling equation, for getting

nonlinear buckling load, generally the nonlinear terms are neglected [20]. However, in this study for obtaining the most accurate nonlinear buckling load, the nonlinear terms of buckling equation are not omitted.

2. THE GOVERNING EQUATION

Figure 1 shows the circular graphene. Based on the first-order shear deformation theory, the displacement field is defined as Equation (1) [25]:

$$\begin{aligned} u(r, \theta, z) &= u_0(r) + z\varphi_r; v(r, \theta, z) = 0; \\ w(r, \theta, z) &= w_0(r) \end{aligned} \quad (1)$$

where, u , v and w , are displacement components of each point at a distance z from the median plane in the directions of r , θ and z , respectively. Displacement components at the median plane, are u_0 and w_0 , which are the functions of variable r . Also, φ_r is the rotation about θ .

Nonlinear strain-displacement relations are obtained based on von Karman's assumptions as [25]:

$$\begin{aligned} \varepsilon_r &= \frac{du}{dr} + z \frac{d\varphi}{dr} + \frac{1}{2} \left(\frac{dw}{dr} \right)^2 \\ \varepsilon_\theta &= \frac{u}{r} + z \frac{\varphi}{r}; \varepsilon_{rz} = \frac{1}{2} \left(\frac{dw}{dr} + \varphi \right) \end{aligned} \quad (2)$$

In local continuum mechanics theory, stress at a point relies on strain at the same point, but Eringen revealed that in nonlocal continuum mechanics, stress is dependent on strain in the entire continuum environment. The governing equation of nonlocal continuum mechanics theory is presented by Eringen as follow [8]:

$$\sigma^{NL} - \mu \nabla^2 \sigma^{NL} = \sigma^L \quad (3)$$

μ is nonlocal coefficient. Then, nonlocal stresses using the Equation (3) can be defined in polar coordinates system in general form as follows [26]:

$$\sigma_r^{NL} - \mu \left(\nabla^2 \sigma_r^{NL} - \frac{4}{r^2} \frac{\partial \sigma_r^{NL}}{\partial \theta} - \frac{2}{r^2} (\sigma_r^{NL} - \sigma_\theta^{NL}) \right) = \sigma_r^L \quad (4)$$

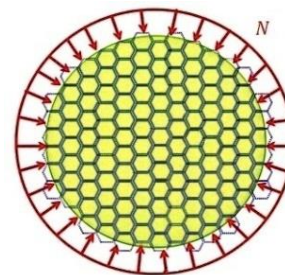


Figure 1. Circular graphene plate under loading

$$\sigma_{\theta}^{NL} - \mu \left(\nabla^2 \sigma_{\theta}^{NL} + \frac{4}{r^2} \frac{\partial \sigma_{r\theta}^{NL}}{\partial \theta} + \frac{2}{r^2} (\sigma_r^{NL} - \sigma_{\theta}^{NL}) \right) = \sigma_{\theta}^L \quad (5)$$

$$\sigma_{r\theta}^{NL} - \mu \left(\nabla^2 \sigma_{r\theta}^{NL} - \frac{4}{r^2} \sigma_{r\theta}^{NL} + \frac{2}{r^2} \frac{\partial}{\partial \theta} (\sigma_r^{NL} - \sigma_{\theta}^{NL}) \right) = \sigma_{r\theta}^L \quad (6)$$

$$\sigma_{rz}^{NL} - \mu \left(\nabla^2 \sigma_{rz}^{NL} - \frac{1}{r^2} \sigma_{rz}^{NL} - \frac{2}{r^2} \frac{\partial \sigma_{\theta z}^{NL}}{\partial \theta} \right) = \sigma_{rz}^L \quad (7)$$

$$\left(\sigma_{\theta z}^{NL} - \mu \left(\nabla^2 \sigma_{\theta z}^{NL} - \frac{1}{r^2} \sigma_{\theta z}^{NL} + \frac{2}{r^2} \frac{\partial \sigma_{rz}^{NL}}{\partial \theta} \right) \right) = \sigma_{\theta z}^L \quad (8)$$

In Equations (4-8), ∇^2 is the Laplacian operator in polar coordinates system. σ^{NL} is nonlocal stress tensor and σ^L is the local stress tensor which is described as Equation (9):

$$\sigma^L = C : \varepsilon \quad (9)$$

In this study, graphene sheet is considered as orthotropic and C is stiffness matrix and is determined as Equation (10):

$$C = \begin{bmatrix} \frac{E_1}{(1-\nu_{12}\nu_{21})} & \frac{\nu_{21}E_2}{(1-\nu_{12}\nu_{21})} & 0 \\ \frac{\nu_{12}E_2}{(1-\nu_{12}\nu_{21})} & \frac{E_2}{(1-\nu_{12}\nu_{21})} & 0 \\ 0 & 0 & G_{12} \end{bmatrix} \quad (10)$$

E_1 and E_2 are elasticity modulus in directions 1 and 2, ν_{12} and ν_{21} are Poisson's ratio in pre-mentioned directions and G_{12} the shear modulus. The stress resultants can be defined as follows [8]:

$$(N_r, N_{\theta}, Q_r)^{NL} = \int_{-\frac{h}{2}}^{\frac{h}{2}} (\sigma_r^{NL}, \sigma_{\theta}^{NL}, \sigma_{rz}^{NL}) dz \quad (11)$$

$$(M_r, M_{\theta})^{NL} = \int_{-\frac{h}{2}}^{\frac{h}{2}} (\sigma_r^{NL}, \sigma_{\theta}^{NL}) z dz \quad (12)$$

h is the thickness of graphene. To determine the equilibrium equations, the principle of minimum potential energy is used:

$$\Pi = U + \Omega \quad (13)$$

where, Π is the total potential energy of the system, U is strain energy and Ω is potential energy of the system of external loads. According to this principle, when the system is in equilibrium, variations in potential energy of the system is zero:

$$\delta \Pi = \delta U + \delta \Omega \cong 0 \quad (14)$$

The strain energy variations of the system and the potential energy of external loads [19] are determined as Equations (15) and (16):

$$U = \frac{1}{2} \int_{-\frac{h}{2}}^{\frac{h}{2}} \int_0^{2\pi} \int_0^r \sigma_{ij}^{NL} \varepsilon_{ij} r dr d\theta dz = \frac{1}{2} \int_{-\frac{h}{2}}^{\frac{h}{2}} \int_0^{2\pi} \int_0^r (\sigma_r^{NL} \varepsilon_{rr} + \sigma_{\theta}^{NL} \varepsilon_{\theta\theta} + \sigma_{r\theta}^{NL} \varepsilon_{r\theta} + \sigma_{rz}^{NL} \varepsilon_{rz} + \sigma_{\theta z}^{NL} \varepsilon_{\theta z}) r dr d\theta dz \quad (15)$$

$$\Omega = - \int_{-\frac{h}{2}}^{\frac{h}{2}} \int_0^{2\pi} \int_0^r N \left(\frac{d(ru_r)}{dr} + \frac{du_{\theta}}{d\theta} \right) r dr d\theta dz \quad (16)$$

where, N is radial in-plane load. The potential energy of elastic foundation is as the form of Equation (17) [27]:

$$V_w = \frac{1}{2} \int_A kw^2 dA \quad (17)$$

where, k is the coefficient of elastic foundation. Using the above equation, the equilibrium equations in terms of the nonlocal stress resultant are obtained as Equations (18-20):

$$\delta u : N_r^{NL} - r \frac{dN_r^{NL}}{dr} + N_{\theta}^{NL} + N = 0 \quad (18)$$

$$\delta \varphi : -r \frac{dM_r^{NL}}{dr} + M_{\theta}^{NL} + rQ_r^{NL} - M_r^{NL} = 0 \quad (19)$$

$$\delta w : Q_r^{NL} + r \frac{dQ_r^{NL}}{dr} + \frac{d}{dr} (rN_r^{NL} \frac{dw}{dr}) - kw = 0 \quad (20)$$

Using Equation (3), the equilibrium equations in terms of local stress resultants are obtained from Equations (21-23):

$$-N_r^L - r \frac{dN_r^L}{dr} + N_{\theta}^L + N = 0 \quad (21)$$

$$-r \frac{dM_r^L}{dr} + M_{\theta}^L + rQ_r^L - M_r^L = 0 \quad (22)$$

$$Q_r^L + r \frac{dQ_r^L}{dr} + (1 - \mu \nabla^2) \left[\frac{d}{dr} (rN_r^L \frac{dw}{dr}) - kw \right] = 0 \quad (23)$$

Relationships with local stress resultant in terms of displacement are:

$$\begin{aligned}
 N_r^L &= A_{11} \left(\frac{du_0}{dr} + \frac{1}{2} \left(\frac{dw}{dr} \right)^2 \right) + A_{12} \left(\frac{u_0}{r} \right); \\
 N_\theta^L &= A_{12} \left(\frac{du_0}{dr} + \frac{1}{2} \left(\frac{dw}{dr} \right)^2 \right) + A_{22} \left(\frac{u_0}{r} \right); \\
 Q_r^L &= A_{33} \left(\frac{dw}{dr} \right); M_r^L = D_{11} \left(\frac{d\varphi}{dr} \right) + D_{12} \left(\frac{\varphi}{r} \right); \\
 M_\theta^L &= D_{12} \left(\frac{d\varphi}{dr} \right) + D_{22} \left(\frac{\varphi}{r} \right)
 \end{aligned}
 \tag{24}$$

The coefficients of these equations are:

$$\begin{aligned}
 A_{11} &= \frac{E_1 h}{(1-\nu_{12}\nu_{21})}, \quad A_{12} = \frac{\nu_{12} E_2 h}{(1-\nu_{12}\nu_{21})}, \quad A_{33} = \frac{5}{6} (G_{12}) h, \\
 D_{11} &= \frac{E_1 h^3}{12(1-\nu_{12}\nu_{21})}, \quad D_{22} = \frac{E_2 h^3}{12(1-\nu_{12}\nu_{21})}, \quad D_{12} = \frac{\nu_{12} E_2 h^3}{12(1-\nu_{12}\nu_{21})}
 \end{aligned}
 \tag{25}$$

Using Equations (24) and (25), the equilibrium Equations (21-23) based on the displacement are obtained as the Equations (26-28):

$$\begin{aligned}
 &A_{11} \left(\frac{du_0}{dr} + \frac{1}{2} \left(\frac{dw}{dr} \right)^2 \right) + A_{12} \left(\frac{u_0}{r} \right) + \\
 &r A_{11} \left(\frac{d^2 u_0}{dr^2} + \frac{d^2 w}{dr^2} \frac{dw}{dr} \right) + A_{12} \left(\frac{du_0}{dr} \right) - \\
 &A_{12} \frac{u_0}{r} - A_{12} \left(\frac{du_0}{dr} + \frac{1}{2} \left(\frac{dw}{dr} \right)^2 \right) \\
 &= 0
 \end{aligned}
 \tag{26}$$

$$-r D_{11} \frac{d^2 \varphi}{dr^2} + D_{22} \left(\frac{\varphi}{r} \right) + r A_{33} \left(\frac{dw}{dr} \right) - D_{11} \left(\frac{d\varphi}{dr} \right) = 0
 \tag{27}$$

$$\begin{aligned}
 &r \left(A_{11} \left(\frac{du_0}{dr} + \frac{1}{2} \left(\frac{dw}{dr} \right)^2 \right) + A_{12} \left(\frac{u_0}{r} \right) \right) \frac{d^2 w}{dr^2} + \\
 &(A_{11} \left(\frac{du_0}{dr} + \frac{1}{2} \left(\frac{dw}{dr} \right)^2 \right) + A_{12} \left(\frac{u_0}{r} \right)) \frac{dw}{dr} + \\
 &r \left[A_{11} \left(\frac{d^2 u_0}{dr^2} + \frac{d^2 w}{dr^2} \frac{dw}{dr} \right) + A_{12} \left(\frac{-u_0}{r^2} + \right. \right. \\
 &\left. \left. \frac{1}{r} \frac{du_0}{dr} \right) \right] \left(\frac{dw}{dr} \right) + A_{33} \left(\frac{dw}{dr} \right) + r A_{33} \frac{d^2 w}{dr^2} + \\
 &(1-\mu\bar{\nu}^2) \left[(N_{cr} \left(r \frac{d^2 w}{dr^2} + \frac{dw}{dr} \right) - kw) \right] = 0
 \end{aligned}
 \tag{28}$$

Here, for buckling analysis, adjacent equilibrium method is used. The equilibrium equation can be obtained from the very small variations near equilibrium state. Therefore, the displacements are considered as follows:

$$u = u^0 + u^1; \quad w = w^0 + w^1; \quad \varphi = \varphi^0 + \varphi^1
 \tag{29}$$

where, in above relations the superscript 0 is for the pre-buckling state and superscript 1 induced very small changes in steady state. By solving pre-buckling equations, it can be concluded:

$$N_r^0 = N_\theta^0 = -N
 \tag{30}$$

Furthermore, stability equations are obtained as Equations (31-33):

$$-N_r^1 - r \frac{dN_r^1}{dr} + N_\theta^1 = 0
 \tag{31}$$

$$-r \frac{dM_r^1}{dr} + M_\theta^1 + r Q_r^1 - M_r^1 = 0
 \tag{32}$$

$$\begin{aligned}
 &Q_r^1 + r \frac{dQ_r^1}{dr} + (1-\mu\bar{\nu}^2) \left[(N_r^0 \frac{dw^1}{dr}) + \right. \\
 &(N_r^1 \frac{dw^1}{dr}) + r \frac{dN_r^0}{dr} \left(\frac{dw^1}{dr} \right) + r \frac{dN_r^1}{dr} \left(\frac{dw^1}{dr} \right) + \\
 &\left. r N_r^0 \frac{d^2 w^1}{dr^2} + r N_r^1 \frac{d^2 w^1}{dr^2} - kw^1 \right] = 0
 \end{aligned}
 \tag{33}$$

In order to obtain non-dimensional stability equation, non-dimensional expressions are defined as:

$$\begin{aligned}
 r^* &= \frac{r}{r_0}, \quad u^* = \frac{u}{h}, \quad w^* = \frac{w}{r_0}, \quad \varphi = \varphi^*, \quad \gamma = \frac{r}{h_0} \\
 (A_{11}, A_{12}, A_{33}) &= \frac{(\bar{A}_{11}, \bar{A}_{12}, \bar{A}_{33})}{Eh} \\
 \bar{N} &= \frac{NR^2}{D}, \quad D = \frac{Eh^3}{12(1-\nu^2)}, \quad \bar{k} = \frac{kr^4}{D}
 \end{aligned}
 \tag{34}$$

Non-dimensional stability equations in terms of displacement are obtained as Equations (35-37):

$$\begin{aligned}
 &\frac{d^2 u_0^*}{dr^{*2}} (r^* \bar{A}_{11}) + \frac{du_0^*}{dr^*} (\bar{A}_{11}) + \frac{u_0^*}{r^*} (-\bar{A}_{22}) + \\
 &\frac{d^2 w^*}{dr^{*2}} \left(\frac{dw^*}{dr^*} \bar{A}_{11} r^* \gamma \right) + \frac{dw^*}{dr^*} \cdot \frac{\gamma}{2} (\bar{A}_{11} - \bar{A}_{12}) = 0
 \end{aligned}
 \tag{35}$$

$$\begin{aligned}
 &-r^* \bar{D}_{11} \frac{d^2 \varphi^*}{dr^{*2}} + \bar{D}_{22} \left(\frac{\varphi^*}{r^*} \right) + r^* \bar{A}_{33} \left(\frac{dw^*}{dr^*} \right) - \\
 &\bar{D}_{11} \left(\frac{d\varphi^*}{dr^*} \right) = 0
 \end{aligned}
 \tag{36}$$

$$\begin{aligned}
 &r^* \bar{A}_{11} \left(\frac{du_0^*}{dr^*} + \frac{\gamma}{2} \left(\frac{dw^*}{dr^*} \right)^2 \right) + \bar{A}_{12} \left(\frac{u_0^*}{r^*} \right) \frac{d^2 w^*}{dr^{*2}} \\
 &+ (\bar{A}_{11} \left(\frac{du_0^*}{dr^*} + \frac{\gamma}{2} \left(\frac{dw^*}{dr^*} \right)^2 \right) + \bar{A}_{12} \left(\frac{u_0^*}{r^*} \right)) \frac{dw^*}{dr^*} + \\
 &r^* \bar{A}_{11} \left(\frac{d^2 u_0^*}{dr^{*2}} + \frac{\gamma}{2} \left(\frac{d^2 w^*}{dr^{*2}} \frac{dw^*}{dr^*} \right) \right) + \bar{A}_{12} \left[\frac{-u_0^*}{r^*} \right. \\
 &\left. + \frac{1}{r^*} \frac{du_0^*}{dr^*} \right] \left(\frac{dw^*}{dr^*} \right) + \gamma \bar{A}_{33} \left(\frac{dw^*}{dr^*} \right) + \\
 &r^* \gamma \bar{A}_{33} \frac{d^2 w^*}{dr^{*2}} + \gamma (1-\mu\bar{\nu}^2) \left[(\bar{N} (r^* \frac{d^2 w^*}{dr^{*2}} + \right. \\
 &\left. \frac{dw^*}{dr^*}) - w^* \bar{k} \right] = 0
 \end{aligned}
 \tag{37}$$

3. DIFERENTIAL QUADRATURE METHOD

In the differential quadrature method, a partial derivative of a function can be written as the linear sum of the functional values at all grid points in the whole zone and can be expressed as the Equation (38) [21, 28]:

$$\frac{d^n F}{dr^n} = \sum_{j=1}^N C_{ij}^{(n)} F(r_j) \tag{38}$$

So that $C_{ij}^{(n)}$, is the weight coefficient and the first order derivative is obtained as follows:

$$c_{ij}^{(1)} = \frac{p(r_i)}{(r_i - r_j)p(r_j)}, p(r_i) = \prod_{\substack{k=1 \\ k \neq i}}^N (r_i - r_k), i \neq j \tag{39}$$

$$C_{ij}^{(1)} = - \sum_{\substack{k=1, \neq i \\ i=1, 2, \dots, N}}^N C_{ki}^{(n)}, i \neq j \tag{40}$$

For instance, the discretize form of Equation (35) is as follows:

$$\begin{aligned} & \bar{A}_{11} \left(\sum_{j=1}^N r_j^* A_{ij}^{(2)} u_{0j} \right) + \bar{A}_{11} \left(\sum_{j=1}^N A_{ij}^{(1)} u_{0j} \right) + \\ & (\gamma \bar{A}_{11}) \left(\sum_{j=1}^N A_{ij}^{(2)} w_j \right) \left(\sum_{j=1}^N r_j^* A_{ij}^{(1)} w_j \right) + \\ & - \bar{A}_{22} \sum_{j=1}^N \frac{u_{0j}}{r_j^*} + (\bar{A}_{11} - \bar{A}_{12}) \frac{\gamma}{2} \left(\sum_{j=1}^N A_{ij}^{(1)} w_j \right) = 0 \end{aligned} \tag{41}$$

4. NUMERICAL RESULTS

To determine the numerical results, an orthotropic circular single layer with radius $r = 5nm$, thickness $h = 0.34nm$, elasticity modulus $E_1 = 1765GPa/nm$, $E_2 = 1588GPa/nm$ and Poisson coefficient $\nu_{12} = 0.3$ is considered [20].

Because the result of numerical differential quadrature method is dependent on the number of nodes, the convergence results of the present study is illustrated in Figure 2. As can be seen, the desired convergence is achieved after 9 nodes.

First to check the accuracy of the results and compare with other references and because there is not any other published paper for the nonlinear symmetric orthotropic buckling of circular nanoplates using the nonlocal elasticity theory so far, the problem is solved for isotropic state with linear strains. In order to validate, buckling strain ($\epsilon_b(\%)$) is defined as follow [24]:

$$\epsilon_b = \frac{N}{Eh} = \frac{\bar{N}h^2}{12(1-\nu^2)r^2} \tag{42}$$

So, the comparison of present study with reference[24] in clamped condition, is examined in Table 1. As can be seen, Table 1 illustrates good harmony.

For comparison in the case of non-linear and linear non-dimensional buckling loads, the variable Rs is defined as follow:

$$Rs = \frac{\text{non - linear non - dimensional buckling load}}{\text{linear non - dimensional buckling load}}$$

Figure 3 shows the changes of non-dimensional buckling loads in non-linear and linear state to nonlocal parameters without elastic foundation for clamped and simply support conditions. The idea of obtaining nonlinear results, is similar to the approach in [29]. It can be seen that the effect of nonlinear analysis in clamped condition is significantly higher and by increasing nonlocal parameters, the differences in results of these two analyses are increased.

Figure 4 illustrates the variations of non-dimensional buckling loads with/without nonlinear terms in the stability equation and without elastic foundation in clamped and simply support conditions. To compare the non-dimensional buckling loads in the presence, with the absence of nonlinear terms in the buckling equation, the variable Rd is defined as follow:

$$Rd = \frac{\text{buckling loads without nonlinear terms}}{\text{buckling loads with nonlinear terms}}$$

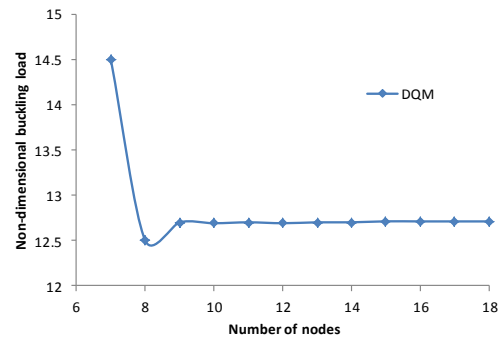


Figure 2. Convergence study of non-dimension buckling load based on the number of nodes

TABLE 1. The comparison of buckling strain for isotropic circular linear isotropic nano plate with[24]

Radius	Buckling strain ($\epsilon_b(\%)$)				
	Nonlocal parameter ($\mu=(e_0 a)^2$)				
	0	0.25	1	2.25	4
4	0.916	0.745	0.447	0.222	0.125
4[24]	0.943	0.767	0.491	0.307	0.202
6	0.413	0.375	0.293	0.215	0.157
6[24]	0.419	0.380	0.297	0.218	0.159
8	0.234	0.221	0.190	0.154	0.122
8[24]	0.235	0.223	0.191	0.155	0.123
10	0.150	0.144	0.130	0.112	0.094
10[24]	0.150	0.145	0.131	0.113	0.095

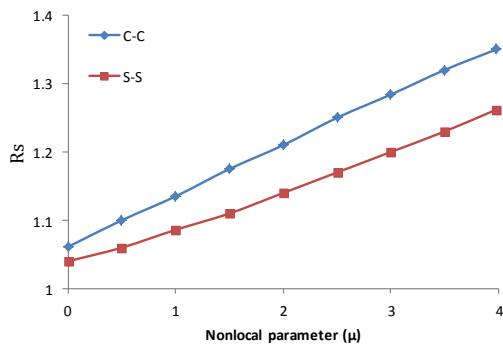


Figure 3. Changes of Rs for different non-local parameters in simply and clamped boundary conditions ($k^- = 0$)

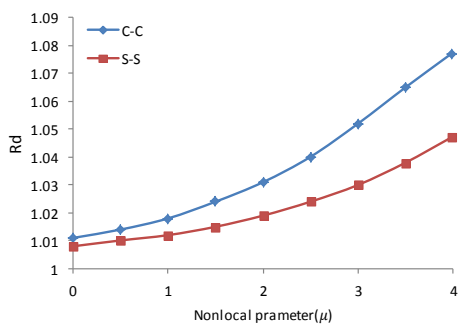


Figure 4. Rd for different non-local parameters in simply and clamped boundary conditions ($k^- = 0$)

It can be noticed from Figure 4, that differences of calculating the nonlinear buckling load, with/without nonlinear terms in buckling equation are relatively noticeable. Moreover, in clamped condition with increasing nonlocal parameters, by neglecting nonlinear terms in stability equations, cause some errors in the actual results.

In Figure 5 the variations of the non-dimensional buckling loads for various nonlocal coefficients with different values of elastic foundations are plotted. It can be observed that with increasing stiffness of elastic foundation the non-dimensional buckling loads increase. In other words, the enhancement of elastic foundation rigidity leads to increase structural stiffness effects and decrease the nonlocal parameter effect on non-dimensional buckling loads. The impact of elastic foundation stiffness in clamped condition is higher than in simply support condition. It can be noticed that by the increase of nonlocal parameters, the non-dimensional buckling loads converge to almost a certain value. To compare the non-dimensional buckling loads in the presence with absence of elastic foundation, the variable Rf is defined as follow:

$$Rf = \frac{\text{non - dimensional buckling loads}(k^- = 1)}{\text{non - dimensional buckling loads}(k^- = 0)}$$

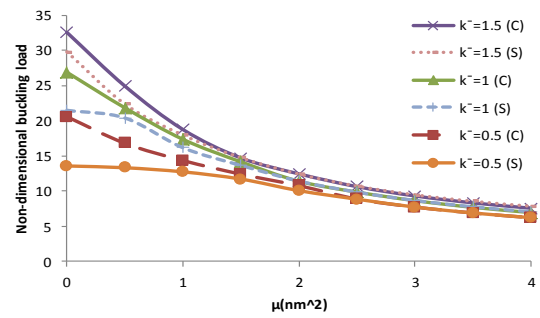


Figure 5. Non-dimensional buckling loads to nonlocal parameters for different elastic coefficients

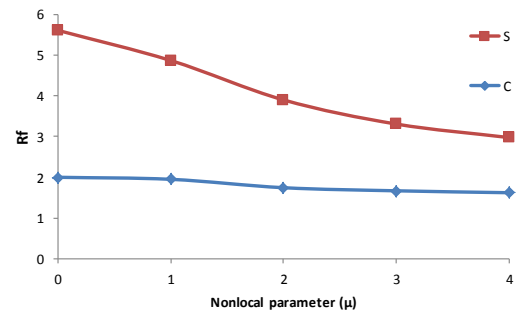


Figure 6. Rf for different non-local parameters in simply and clamped boundary conditions

As can be seen from Figure 6, by increasing nonlocal parameters, Rf reduces and its values are higher in simply support condition rather than clamped condition. Moreover, by increasing nonlocal parameter, the values of clamped and simply support boundary conditions are got near to each other.

Figure 7 indicates the changes of non-dimensional buckling loads to non-dimensional radius, for different nonlocal parameters in clamped and simply support conditions.

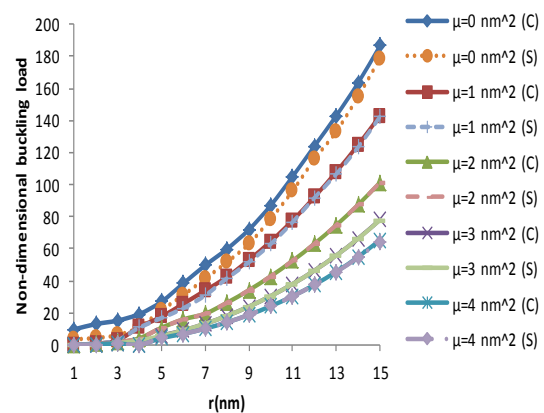


Figure 7. Non-dimensional buckling loads to radius, for various nonlocal coefficients in clamped and simply support conditions ($k^- = 1$)

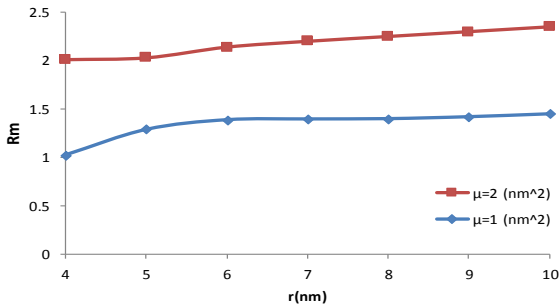


Figure 8. R_m to radius in simply support condition

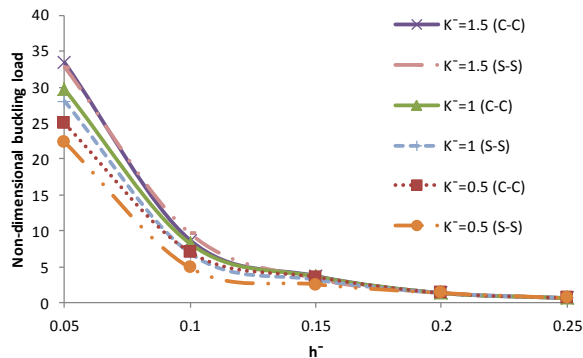


Figure 9. Non-dimensional buckling loads to non-dimensional thickness, for different elastic foundation coefficients in clamped and simply support conditions.

It is noticeable that by the increase of radius, the non-dimensional buckling loads increase, too. To examine the differences between local and nonlocal theory, the variable R_m is defined as follow:

$$R_m = \frac{\text{local non - dimensional buckling loads}}{\text{nonlocal non - dimensional buckling loads}}$$

In Figure 8, the changes of non-dimensional buckling loads in the local to nonlocal state are plotted in $\mu = 1, 2 \text{ nm}^2$ for different radii in simply support condition. It can be seen that, as radius increases, the difference between the theoretical buckling results of local and nonlocal gets further.

The changes of the non-dimensional buckling loads to the non-dimensional thickness for different elastic foundation coefficients in clamped and simply support conditions are illustrated in Figure 9. According to the graph, as the non-dimensional thickness increases, the non-dimensional buckling load reduces. Also, in a certain non-dimensional thickness, as elastic foundation rigidity gets higher for the same values of elastic foundation, the non-dimensional buckling load increases. By increasing the thickness, the surface effect disappears. The reason for this phenomenon is that with increasing thickness, surface to volume ratio of the structure gets lower. Thus, it can neglect the energy

level to the total amount of energy which the classic theory fails to predict such behavior [19].

5. DISCUSSION AND CONCLUSIONS

In this paper, nonlinear buckling analysis of circular graphene plates with nonlocal elasticity theory is analyzed. In this study, for getting the most accurate data, nonlinear terms of the stability equation, are considered. The most important results are as follows:

- The effect of nonlocal parameter on simply support condition is less than clamped condition.
- The increase of nonlocal parameter, reduces the non-dimensional buckling load.
- In the case of using nonlinear terms or only linear terms of the stability equation, by the increase of nonlocal parameter, the difference in results increases. In other words, by the increase of nonlocal parameter, the importance of nonlinear terms in calculating non-dimensional buckling load increases.
- By increasing non-dimensional radius, the difference of results between local and nonlocal analyses, increase.
- For getting the most accurate buckling load, in nonlinear buckling analyses, it is highly recommended to not omit nonlinear terms in buckling equation, because the results are relatively different.

6-REFERENCES

1. Iijima, S., "Helical microtubules of graphitic carbon", *Nature*, Vol. 354, No. 6348, (1991), 56-58.
2. Ma, M., Tu, J., Yuan, Y., Wang, X., Li, K., Mao, F. and Zeng, Z., "Electrochemical performance of ZnO nanoplates as anode materials for Ni/Zn secondary batteries", *Journal of Power Sources*, Vol. 179, No. 1, (2008), 395-400.
3. Yguerabide, J. and Yguerabide, E.E., "Resonance light scattering particles as ultrasensitive labels for detection of analytes in a wide range of applications", *Journal of Cellular Biochemistry*, Vol. 84, No. S37, (2001), 71-81.
4. Aagesen, M. and Sorensen, C., "Nanoplates and their suitability for use as solar cells", *Proceedings of Clean Technology*, (2008), 109-112.
5. Chiu, H.-Y., Hung, P., Postma, H.W.C. and Bockrath, M., "Atomic-scale mass sensing using carbon nanotube resonators", *Nano letters*, Vol. 8, No. 12, (2008), 4342-4346.
6. Hernandez, E., Goze, C., Bernier, P. and Rubio, A., "Elastic properties of C and BxCyNz composite nanotubes", *Physical Review Letters*, Vol. 80, No. 20, (1998), 4502-4505.
7. Peng, J., Wu, J., Hwang, K., Song, J. and Huang, Y., "Can a single-wall carbon nanotube be modeled as a thin shell?", *Journal of the Mechanics and Physics of Solids*, Vol. 56, No. 6, (2008), 2213-2224.
8. Eringen, A.C., "Nonlocal continuum field theories", Springer Science & Business Media, (2002).
9. Shahidi A. R., Anjomshoa A., Shahidi S. H. and RaeesiEstabragh E., "Nonlocal effect on buckling of triangular nanocomposite plates", *International Journal of Engineering, Transaction C: Aspects*, Vol. 29, No. 3, (2016), 411-425.

10. Amiri, A., Fakhari, S., Pournaki, I., Rezazadeh, G. and Shabani, R., "Vibration analysis of circular magneto-electro-elastic nanoplates based on eringen's nonlocal theory", *International Journal of Engineering-Transactions C: Aspects*, Vol. 28, No. 12, (2015), 1808-1817.
11. Pradhan, S. and Murmu, T., "Small scale effect on the buckling of single-layered graphene sheets under biaxial compression via nonlocal continuum mechanics", *Computational Materials Science*, Vol. 47, No. 1, (2009), 268-274.
12. Samaei, A., Abbasion, S. and Mirsayar, M., "Buckling analysis of a single-layer graphene sheet embedded in an elastic medium based on nonlocal mindlin plate theory", *Mechanics Research Communications*, Vol. 38, No. 7, (2011), 481-485.
13. Farajpour, A., Danesh, M. and Mohammadi, M., "Buckling analysis of variable thickness nanoplates using nonlocal continuum mechanics", *Physica E: Low-dimensional Systems and Nanostructures*, Vol. 44, No. 3, (2011), 719-727.
14. Farajpour, A., Shahidi, A., Mohammadi, M. and Mahzoon, M., "Buckling of orthotropic micro/nanoscale plates under linearly varying in-plane load via nonlocal continuum mechanics", *Composite Structures*, Vol. 94, No. 5, (2012), 1605-1615.
15. Emam, S.A., "A general nonlocal nonlinear model for buckling of nanobeams", *Applied Mathematical Modelling*, Vol. 37, No. 10, (2013), 6929-6939.
16. Mohammadi, M., Farajpour, A., Moradi, A. and Ghayour, M., "Shear buckling of orthotropic rectangular graphene sheet embedded in an elastic medium in thermal environment", *Composites Part B: Engineering*, Vol. 56, (2014), 629-637.
17. Sarrami-Foroushani, S. and Azhari, M., "Nonlocal vibration and buckling analysis of single and multi-layered graphene sheets using finite strip method including van der waals effects", *Physica E: Low-dimensional Systems and Nanostructures*, Vol. 57, (2014), 83-95.
18. Ravari, M.K. and Shahidi, A., "Axisymmetric buckling of the circular annular nanoplates using finite difference method", *Meccanica*, Vol. 48, No. 1, (2013), 135-144.
19. Bedroud, M., Hosseini-Hashemi, S. and Nazemnezhad, R., "Buckling of circular/annular mindlin nanoplates via nonlocal elasticity", *Acta Mechanica*, Vol. 224, No. 11, (2013), 2663-2676.
20. Golmakani, M. and Rezatalab, J., "Nonuniform biaxial buckling of orthotropic nanoplates embedded in an elastic medium based on nonlocal mindlin plate theory", *Composite Structures*, Vol. 119, (2015), 238-250.
21. Dastjerdi, S. and Jabbarzadeh, M., "A non-linear static equivalent model for multi-layer annular/circular graphene sheet based on non-local elasticity theory considering third order shear deformation theory in thermal environment", *International Journal of Engineering-Transactions A: Basics*, Vol. 28, No. 10, (2015), 1533-1542.
22. Dastjerdi, S. and Jabbarzadeh, M., "Nonlinear bending analysis of bilayer orthotropic graphene sheets resting on winker-pasternak elastic foundation based on non-local continuum mechanics", *Composites Part B: Engineering*, Vol. 87, (2016), 161-175.
23. Dastjerdi, S., Jabbarzadeh, M. and Aliabadi, S., "Nonlinear static analysis of single layer annular/circular graphene sheets embedded in winker-pasternak elastic matrix based on non-local theory of eringen", *Ain Shams Engineering Journal*, (2016).
24. Farajpour, A., Mohammadi, M., Shahidi, A. and Mahzoon, M., "Axisymmetric buckling of the circular graphene sheets with the nonlocal continuum plate model", *Physica E: Low-dimensional Systems and Nanostructures*, Vol. 43, No. 10, (2011), 1820-1825.
25. Nosier, A. and Fallah, F., "Non-linear analysis of functionally graded circular plates under asymmetric transverse loading", *International Journal of Non-linear Mechanics*, Vol. 44, No. 8, (2009), 928-942.
26. Dastjerdi, S., Jabbarzadeh, M. and Tahani, M., "Nonlinear bending analysis of sector graphene sheet embedded in elastic matrix based on nonlocal continuum mechanics", *International Journal of Engineering-Transactions B: Applications*, Vol. 28, No. 5, (2015), 802-811.
27. Naderi, A. and Saidi, A., "Exact solution for stability analysis of moderately thick functionally graded sector plates on elastic foundation", *Composite Structures*, Vol. 93, No. 2, (2011), 629-638.
28. Shu, C., "Differential quadrature and its application in engineering", Springer Science & Business Media, (2012).
29. Vosoughi, A., Malekzadeh, P., Banan, M.R. and Banan, M.R., "Thermal postbuckling of laminated composite skew plates with temperature-dependent properties", *Thin-walled Structures*, Vol. 49, No. 7, (2011), 913-922.

Nonlinear Buckling of Circular Nano Plates on Elastic Foundation

M. Jabbarzadeh, M. Sadeghian

Department of Mechanical Engineering, Mashhad Branch, Islamic Azad University, Mashhad, Iran

چکیده

PAPER INFO

Paper history:

Received 03 July 2015

Received in revised form 24 February 2016

Accepted 04 March 2016

Keywords:

Nonlinear Buckling

Circular

Orthotropic

Nonlocal Elasticity

Differential Quadrature Method

در این مقاله، تحلیل غیرخطی کماتش متقارن صفحات نسبتاً ضخیم دایروی گرافن با خواص ارتوتروپیک تحت بار مکانیکی مورد بررسی قرار می‌گیرد. به کمک تئوری الاستیسیته غیرموضعی، اصل کار مجازی، تئوری مرتبه اول برشی و کرنش‌های غیرخطی فون-کارمن، روابط حاکم برحسب جایجایی‌ها بدست آمده و از روش مربعات دیفرانسیلی (DQ) حل شده است. در این تحلیل برای حل معادلات کماتش، از شرایط تعادل همسایگی استفاده شده است. معمولاً، در تحلیل‌های غیرخطی کماتش، جهت بدست آوردن نیروی کماتش، از عبارات‌های غیرخطی به وجود آمده در معادله پایداری صرف‌نظر می‌شود، اما در این مطالعه برای داشتن بیشترین دقت در نتایج، این عبارات‌ها در نظر گرفته شده و بار بی‌بعد کماتش در دو حالت با در نظر گرفتن یا بدون توجه به این عبارات‌ها محاسبه گردیده و تاثیر عبارات‌های غیرخطی بر نتایج بررسی شده است. جهت اعتبار سنجی، نتایج بدست آمده با نتایج کماتش در مراجع دیگر مقایسه شده و اثرات ضریب غیرموضعی، ضخامت، شعاع و پایه الاستیک، بر بارهای بی‌بعد کماتش مورد بررسی قرار گرفته است و نتایج تحلیل به روش تئوری غیرموضعی و موضعی با یکدیگر مقایسه شده است. از نتایج مشاهده می‌شود تاثیر ضریب غیر موضعی بر روی شرط مرزی مفصلی کمتر از شرط مرزی گیردار است. همچنین با زیاد شدن شعاع صفحه، اختلاف نتایج تحلیل غیرموضعی و موضعی افزایش می‌یابد.

doi: 10.5829/idosi.ije.2016.29.05b.14